JOURNAL OF MATERIALS SCIENCE 30 (1995) 1577–1583

A study on martensitic transformation in $Ti_{50-x/2}Ni_{50-x/2}Cu_x$ alloys with $X \leq 10$ at %

Y. C. LO, S. K. WU
Institute of Materials Science and Engineering, National Taiwan University, Taipei, Taiwan, 106, Republic of China

The effect of Cu additions on the martensitic transformation sequence and temperature in $Ti_{50-x/2}Ni_{50-x/2}Cu_x$ alloys with x: 1–10 at% are investigated by ER, DSC, X-ray and IF measurements. Experimental results show that the transformation sequence of $Ti_{50-x/2}Ni_{50-x/2}Cu_x$ alloys with x: 1–4 at% proceeding as two-stage B2 → R → B19′ transformation on cooling and $Ti_{50-x/2}Ni_{50-x/2}Cu_x$ alloys with $x = 5$, 10 at% have no martensitic transformation. The addition of Cu in $Ti_{50-x/2}Ni_{50-x/2}Cu_x$ alloys assists the formation of R-phase, a behaviour which is quite different from that in $Ti_{50}Ni_{50-x}Cu_x$ alloys. Both the *Ms* and T_R temperatures decrease rapidly with increasing Cu addition in $Ti_{50-x/2}Ni_{50-x/2}Cu_x$ alloys with x: 1–4 at%. It is proposed that the Cu + Ni effects on the *Ms* temperature in $Ti_{50-x/2}Ni_{50-x/2}Cu_x$ alloys is similar as Cu + Ni effects in $Ti_{50}Ni_{50-x}Cu_x$ alloys and as Ni effects in as-quenched Ni-rich TiNi alloys.

1. Introduction

There have been many investigations of the effect of ternary Cu addition on the martensitic transformation behaviour in $Ti_{50}Ni_{50-x}Cu_x$ alloys [1–17], such as its effect on shape memory effect [1–4], Ms transformation temperature [5–9], mechanical properties [10–13] and transformation sequence [14–18]. Previous studies have shown that, in $Ti_{50}Ni_{50-x}Cu_x$ alloys, the sensitivity of Ms temperature to composition can be reduced [1, 10, 12]. At the same time, a narrower hysteresis associated with lower martensitic yield strength can be obtained [8–12], and the R-phase can be suppressed [2, 4, 14] in these alloys. Very recently, Nam *et al.* [14–17] have reported that in $Ti_{50}Ni_{50-x}Cu_x$ alloys the transformation sequences of martensitic transformation change significantly with respect to Cu content as following: in the alloys with Cu concentration less than 5 at %, B2 ↔ B19′ transformation takes place; in the 7.5 at % Cu alloy, both B2 ↔ B19′ and B2 ↔ B19 ↔ B19′ transformations take place; in the alloys with Cu concentration between 10 and 15 at %, B2 ↔ B19 ↔ B19′ transformation takes place; in the 20 at % Cu alloy only B2 ↔ B19 transformation takes place. These different transformation sequences have high potential in engineering applications using $Ti_{50}Ni_{50-x}Cu_x$ shape memory alloys, for example, the transformation hysteresis associated with the B2 ↔ B19 transformation in $Ti_{50}Ni_{50-x}Cu_x$ alloys was reported to be about 15 K [16], which is in between those of the B2 ↔ B19′ and B2 ↔ R transformations occurring in TiNi binary alloys.

When a third element is added in a TiNi alloy, the atoms of this element can be located substitutionally at the sites of Ni and/or Ti atoms. It was reported [19] that the atomic location of Cu in $Ti_{48.5}Ni_{48.5}Cu_3$ alloy exists at both the Ni and Ti atom sites in nearly the same ratio. Since the changes in martensite transformation sequence may possibly originate at the location of the third element and can be affected by the amount of the third element, such as where the transformation sequence of B2 ↔ B19′ of TiNi binary alloy changes to B2 ↔ B19 ↔ B19′ of $Ti_{50}Ni_{40}Cu_{10}$ alloy [18], therefore, one can expect that $Ti_{50-x/2}Ni_{50-x/2}Cu_x$ alloys will have different martensitic transformation behaviour from $Ti_{50}Ni_{50-x}Cu_x$ alloys. It is interesting to know the effect of the addition of Cu on the martensitic transformation sequence in $Ti_{50-x/2}Ni_{50-x/2}Cu_x$ alloys where Cu is substituted for both Ni and Ti. It is noted that earlier studies have examined the martensitic transformation sequence in $Ti_{50}Ni_{50-x}Cu_x$ alloys, but to the best of our knowledge, the $Ti_{50-x/2}Ni_{50-x/2}Cu_x$ alloys have not been investigated intensively previously. The purpose of the present study is to systematically clarify the effect of Cu addition on the martensitic transformation behaviour of $Ti_{50-x/2}Ni_{50-x/2}Cu_x$ alloys with $x = 1 \sim 10$ at %. The characteristics associated with the martensitic transformation of $Ti_{50-x/2}Ni_{50-x/2}Cu_x$ alloys will also be discussed and compared with those of $Ti_{50}Ni_{50-x}Cu_x$ alloys.

2. Experimental procedure

Six different $Ti_{50-x/2}Ni_{50-x/2}Cu_x$ ternary alloys with $x = 1, 2, 3, 4, 5$ and 10 at % were used in this study. Pure titanium (purity 99.7%), pure nickel (purity 99.9%) and pure copper (purity 99.9%), 30 g in weight in total, were prepared by a non-consumable tungsten electrode vacuum arc melter under a controlled

0022–2461

protective argon and Ti-gettered atmosphere. The buttons were melted and remelted at least six times to ensure homogeneity. The weight loss of the buttons was negligible during the melting. The as-melted buttons were hot rolled at 900 °C to about 1 mm thickness. Specimens for electrical resistivity testing, differential scanning calorimetry (DSC) measurement and internal friction (IF) testing were carefully cut from the rolled plate with a low speed diamond saw. These specimens were subsequently solution treated at 1000 °C for 1 h in evacuated quartz tubes and then rapidly quenched into room temperature water.

Martensitic transformation temperatures were measured by using a four-probe electrical resistivity measurement technique and by the DSC method. The temperature range for the electrical resistivity test was from + 100 °C to below − 150 °C. The DSC measurement was conducted with a DuPont 2000 thermal analyser equipped with a quantitative scanning system 910 DSC cell and the cooling accessory LNCAII. Measurements were carried out at temperatures ranging from − 150 °C to + 100 °C under the controlled cooling/heating rate of 10 °C min^{-1}. Heats of transformation (ΔH) were automatically calculated from the areas under the DSC peaks by means of equipment software packages.

IF tests were carried out by using a Sinku-Riko 1500 M/L series inverted torsion pendulum in a temperature ranging from − 170 °C to + 100 °C. The temperature rate was precisely controlled at 2 °C min^{-1} and the test frequency was around 1 Hz. The recording of data was completely automatic and plots of internal friction and frequency versus temperature were done on a digital computer.

X-ray diffraction (XRD) analysis was performed by a Philips PW1710 diffractometer, employing the CuK_α radiation and graphite monochromator at 30 kV and 20 mA. The divergence slit was chosen such that the irradiated area of the specimen did not exceed the specimen size 20 × 14 × 1 mm. The diffracted intensity was recorded in the range of 20 to 100 degree 2θ with a scanning rate of about 0.05° s^{-1}.

3. Experimental results

Fig. 1a–f show the curves of electrical resistivity (ER) versus temperature for $Ti_{50-x/2}Ni_{50-x/2}Cu_x$ alloys with x = 1, 2, 3, 4, 5 and 10 at %, respectively, during the heating and cooling cycles. The ER curves depend clearly on the Cu content and are divided into two categories. The ER curves of Fig. 1a–d all show an abnormal resistivity increase prior to a subsequent drop with decreasing temperature. By contrast, in the alloys containing 5 and 10 at % Cu, the ER curves of Fig. 1e and f are smooth, and no abrupt change of electrical resistivity was observed. It is implied that there is no martensitic transformation in these two alloys. Thus, they were excluded from further study.

Fig. 2a–h show the results of DSC measurement for $Ti_{50-x/2}Ni_{50-x/2}Cu_x$ alloys with x = 1, 2, 3, and 4 at %, respectively, on cooling (a–d) and heating (e–h) cycles. From these figures, one can observe

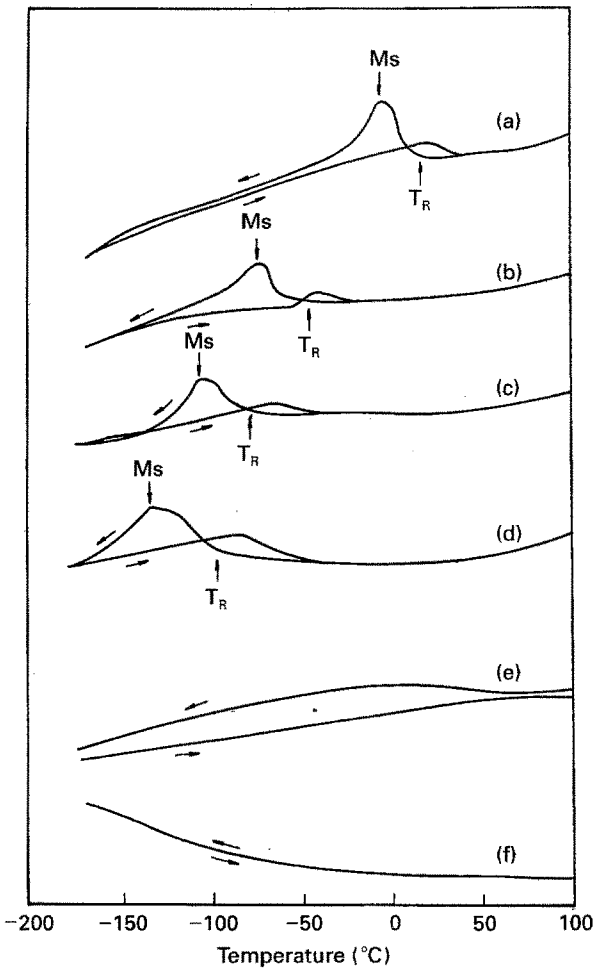

Figure 1 Electrical resistivity versus temperature plots for $Ti_{50-x/2}Ni_{50-x/2}Cu_x$ alloys. (a) x = 1; (b) x = 2; (c) x = 3; (d) x = 4; (e) x = 5; (f) x = 10.

two DSC peaks appearing on cooling curves but only one DSC peak on heating curves. The transformation peak temperatures and ΔH values for each $Ti_{50-x/2}Ni_{50-x/2}Cu_x$ alloy shown in Fig. 2a–h are summarized in Table I. In Table I, ΔH_c, ΔH_c^R and ΔH_h are the ΔH values of peaks M*, R* and A*, respectively.

Fig. 3a–d show experimental results of frequency (shear modulus) and IF spectrum as a function of temperature in $Ti_{50-x/2}Ni_{50-x/2}Cu_x$ alloys at the heating/cooling rate of 2 °C min^{-1}. In these figures, there are two sharp IF peaks for each cooling curve (solid lines) and only one IF peak for each heating curve (dashed lines). All IF peaks correspond to shear modulus minima, as shown in the upper diagrams (frequency versus temperature spectrum) of Fig. 3(a–d).

X-ray diffraction (XRD) was carried out to determine the crystal structure of the parent phase in $Ti_{50-x/2}Ni_{50-x/2}Cu_x$ alloys at room temperature. Fig. 4 shows the typical XRD line profiles of $Ti_{49}Ni_{49}Cu_2$ alloy. The line profiles in Fig. 4 were well fitted for B2 structure and could be indexed to a B2 structure with the lattice parameter a = 0.3037 nm, which is close to that of TiNi binary alloy (a = 0.3015 nm). The XRD line profiles for alloys with x = 1, 3 and 4 at % are all similar to those

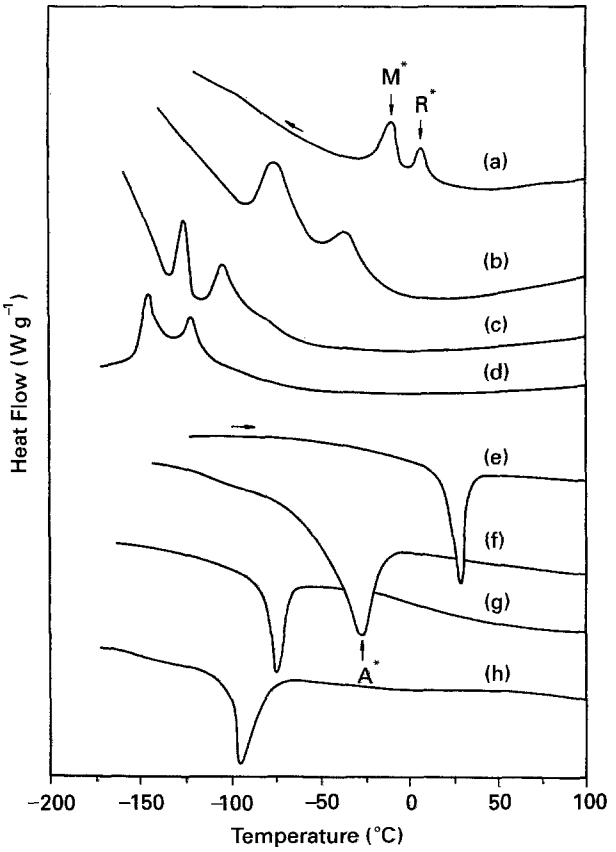

Figure 2 DSC curves for $Ti_{50-x/2}Ni_{50-x/2}Cu_x$ alloys on cooling (a–d) and heating (e–h). (a) $x = 1$; (b) $x = 2$; (c) $x = 3$; (d) $x = 4$; (e) $x = 1$; (f) $x = 2$; (g) $x = 3$; (h) $x = 4$.

in Fig. 4 except that now the lattice parameters are 0.3034 nm, 0.3041 nm and 0.3046 nm, respectively, and thus their X-ray profiles are not shown in this paper. These results immediately mean that Cu addition in $Ti_{50-x/2}Ni_{50-x/2}Cu_x$ alloys with x: 1–4 at % can be fully solid-solutioned into ternary TiNiCu alloys and have the B2 structure in the parent phase. Additionally, from transmission electron microscopy TEM observation conducted elsewhere [20], the bright field image and selected area diffraction patterns also support the X-ray results and reveal only B2 parent phase but no second phase or other precipitates would be formed in $Ti_{50-x/2}Ni_{50-x/2}Cu_x$ alloys with x = 1–4 at %. Oxides were observed in TEM specimens, as has been the case in other binary and ternary TiNi alloys. TEM cold-stage experiments [20] also confirm that the martensite in $Ti_{50-x/2}Ni_{50-x/2}Cu_x$ alloys is B19′ martensite, the same as that of TiNi binary alloys. Hence, from XRD and TEM analysis, the parent phase and martensite were confirmed as fully Cu solid-solutioned B2 and B19′ structures in $Ti_{50-x/2}Ni_{50-x/2}Cu_x$ alloys, respectively.

4. Discussion

4.1. Transformation sequence of $Ti_{50-x/2}Ni_{50-x/2}Cu_x$ alloys

Figs 1–3 clearly indicate that two-stage transformations have occurred on cooling in $Ti_{50-x/2}Ni_{50-x/2}Cu_x$ alloys with x: 1–4 at %, as experimental results of ER, DSC and IF measurements exhibit the abnormal resistivity increase and two DSC peaks as well as two IF peaks. In the following, we will discuss in detail the features shown in Figs 1–3 which demonstrate the characteristics of transformation behaviour occurring in $Ti_{50-x/2}Ni_{50-x/2}Cu_x$ alloys with x: 1–4 at %.

From Fig. 1, it is evident that a resistance increase has occurred prior to the martensite transformation, at which temperature there is a resistance drop with decreasing temperature. This feature is quite analogous to that of $TiNiFe_3$ [21] and $TiNiPd_3$ [22] alloys, which have been confirmed as showing a B2 → R → B19′ transformation sequence on cooling and B19′ → B2 on heating. In view of the similarity in the curves shown in Fig. 1 to those of $TiNiFe_3$ and $TiNiPd_3$ alloys, it is reasonable to suggest that the same transformation sequence also occurs in the $Ti_{50-x/2}Ni_{50-x/2}Cu_x$ alloys with x = 1–4 at %. In other words, Fig. 1a–d exhibit the typical B2 → R → B19′ two-stage martensitic transformation on cooling, where B2, R and B19′ represent cubic, rhombohedral and monoclinic structure, respectively. The notations shown in Fig. 1 for determining transformation temperatures (Ms, T_R etc.) follow the example established by Hwang *et al.* [21]. Comparing the DSC and IF results of Figs 2 and 3 with ER tests of Fig. 1, two DSC peaks and two IF peaks appearing in Fig. 2a–d and Fig. 3a–d are known to be associated with the B2 → R → B19′ martensitic transformation on cooling. Moreover, from Table I, ΔH values associated with B2 → R transformation, i.e. ΔH_c^R, are found to range from 3.11 to 3.74 J g^{-1}, which are located in the corresponding range of the R-phase transformation for $TiNiFe_3$ alloy (3.75 J g^{-1}) [23] and for aged Ni-rich TiNi alloy (1–6 J g^{-1}) [24]. The ΔH_c^R values shown in Table I exhibit the appropriate magnitudes required for the R-phase transformation and also provide the evidence of the B2 → R → B19′ transformation sequence occurring in $Ti_{50-x/2}Ni_{50-x/2}Cu_x$ alloys.

TABLE I DSC measurement of thermal properties for $Ti_{50-x/2}Ni_{50-x/2}Cu_x$ alloys.

x (at %)	M* (°C)	R* (°C)	A* (°C)	A* − M* (°C)	ΔH_c (J g^{-1})	ΔH_c^R (J g^{-1})	ΔH_h (J g^{-1})
1	− 7.47	8.71	28.23	35.7	6.16	3.74	17.68
2	− 71.20	− 34.06	− 25.99	45.2	5.24	3.51	14.15
3	− 121.84	− 98.71	− 75.06	46.8	4.97	3.47	11.42
4	− 140.63	− 115.72	− 94.37	46.3	4.63	3.11	9.87

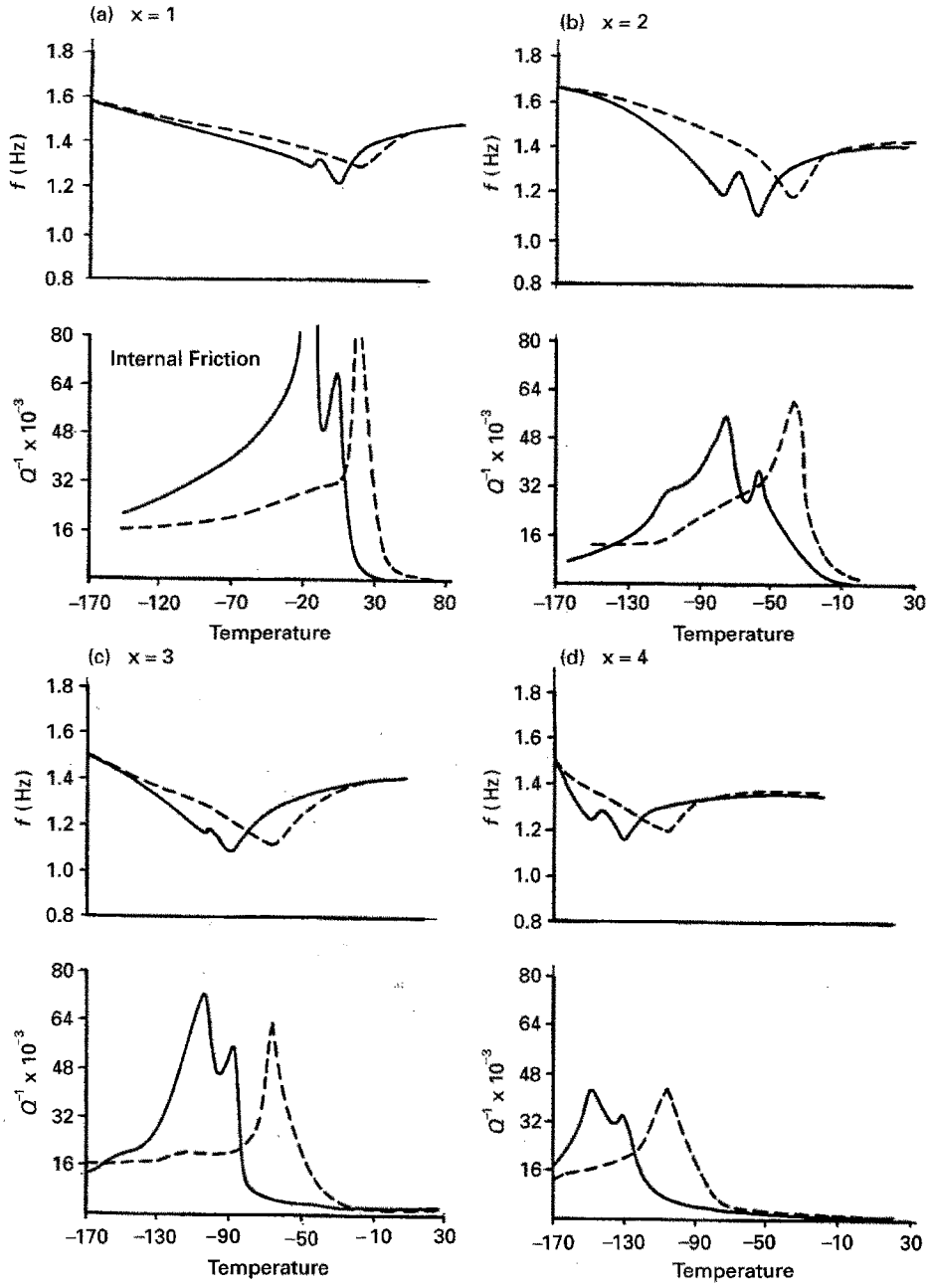

Figure 3 Frequency (f) (shear modulus) and internal friction (Q^{-1}) versus temperature curves for $Ti_{50-x/2}Ni_{50-x/2}Cu_x$ alloys. (—, cooling, – – –, heating; (a) $x = 1$; (b) $x = 2$; (c) $x = 3$; (d) $x = 4$.

By carefully examining the IF results of Fig. 3, two additional points were discovered: (i) from Q^{-1} versus temperature curves, the Q^{-1}_{max} value of B2 → R first-stage transformation is always lower than that of the R → B19′ second stage transformation, and (ii) from frequency versus temperature curves, there are deep minima of frequency (shear modulus) corresponding to the B2 → R first-stage transformation but there are just shallow minima of frequency (shear modulus) corresponding to R → B19′ second-stage transformation. Both IF features mentioned above are consistent with the reported IF results of aged Ni-rich TiNi alloys [25, 26], which had already been proven to exhibit the typical B2 → R → B19′ two-stage transformation. Therefore, the features shown in Fig. 3 can provide additional strong evidence demonstrating the characteristics of B2 → R → B19′ transformation occurring in $Ti_{50-x/2}Ni_{50-x/2}Cu_x$ alloys with x: 1–4 at %.

One may argue that the two-stage transformation in $Ti_{50-x/2}Ni_{50-x/2}Cu_x$ alloys may be regarded as B2 ↔ B19 ↔ B19′ transformation since this transformation sequence had been found in $Ti_{50}Ni_{40}Cu_{10}$ alloy [14, 15, 18]. However, according to our recent investigation on the B2 ↔ B19 ↔ B19′ transformation in $Ti_{50}Ni_{40}Cu_{10}$ alloy [18], B2 ↔ B19 ↔ B19′ transformation possesses the following features of DSC, ER and IF test results: (i) for the DSC curve, there is a large peak for the B2 ↔ B19 transformation but a diffuse peak for the B19 ↔ B19′ transformation, (ii) for the ER diagram, there is a minor resistivity change for B2 ↔ B19 transformation but a significant resistivity change for B19 ↔ B19′ transformation, and (iii) for the IF spectrum, there is a period of frequency (shear

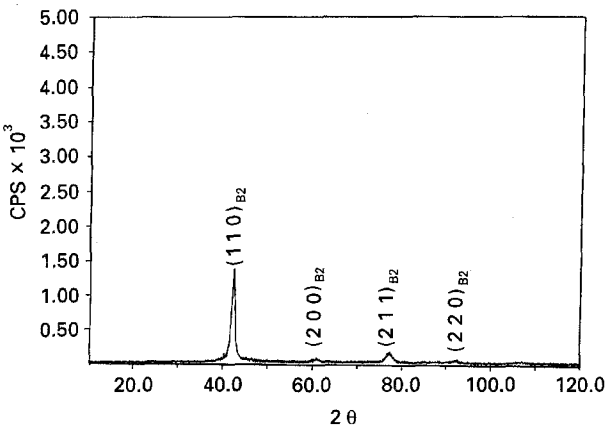

Figure 4 X-ray diffraction line profiles of $Ti_{49}Ni_{49}Cu_2$ alloy at room temperature. All of them show B2 peaks. a_{B2} = 0.3037 nm.

modulus) minimum existing over a wide temperature range between the B2 ↔ B19 and B19 ↔ B19′ transformations. All of the above mentioned three features do not coincide with the results shown in Figs 1–3 of this study. As a result, we excluded the possibility of B2 ↔ B19 ↔ B19′ two-stage transformation occurring in $Ti_{50-x/2}Ni_{50-x/2}Cu_x$ alloys. Consequently, from the above discussions, all evidence supports the view that the martensitic transformation sequence is B2 → R → B19′ in $Ti_{50-x/2}Ni_{50-x/2}Cu_x$ alloys with x: 1–4 at %.

As mentioned above, the transformation sequence of $Ti_{50-x/2}Ni_{50-x/2}Cu_x$ alloys is B2 → R → B19′ on cooling. However, the transformation sequence of well-studied $Ti_{50}Ni_{50-x}Cu_x$ alloys shows no premartensitic R-phase transformation [2, 4, 14]. It has been reported that the transformation sequence in ternary $Ti_{50}Ni_{50-x}Cu_x$ alloys changes considerably as the substitution of Cu is increased [14]: the transformation sequence changes from B2 → B19′ to B2 ↔ B19 ↔ B19′, then to B2 ↔ B19. There is no evidence, however, of a B2 → R → B19′ two-stage transformation sequence occurring in $Ti_{50}Ni_{50-x}Cu_x$ alloys. Hence, $Ti_{50}Ni_{50-x}Cu_x$ alloys do not show the premartensitic R-phase as do $Ti_{50-x/2}Ni_{50-x/2}Cu_x$ alloys, despite the fact that the structures of the high temperature B2 phases and low temperature B19′ martensite are virtually identical when the amount of Cu substitution for both alloy systems is less than 10 at %. The present results of B2 → R → B19′ transformation sequence suggest the addition of Cu in $Ti_{50-x/2}Ni_{50-x/2}Cu_x$ alloys assists the formation of the rhombohedral R-phase. By contrast, the B2 → R → B19′ transformation sequence would be suppressed when the substitution of Cu for Ni in $Ti_{50}Ni_{50-x}Cu_x$ alloys. Reasons for the different transformation sequence in these two alloy systems is not yet completely understood. However, the cause of this phenomenon may be ascribed to different electronic states occurring in these two alloy systems. Since the formation of martensite phase or R-phase which affects the subsequent transformation sequence, may probably originate from some changes in the electronic state caused by different ways of the element addition [27].

One further difference in the transformation behaviour of $Ti_{50-x/2}Ni_{50-x/2}Cu_x$ alloys and $Ti_{50}Ni_{50-x}Cu_x$ alloys is the ER behaviour. In comparing the current results shown in Fig. 1 with those obtained by Nam *et al.* [16], it can be seen that the electrical resistivity change associated with the transformation is very different. That is, in $Ti_{50}Ni_{50-x}Cu_x$ alloys with the B2 → B19′ transformation, the onset of transformation is accompanied by an increase in ER, which is similar to the situation occurring in Cu-based shape memory alloys [28]. Whereas in $Ti_{50-x/2}Ni_{50-x/2}Cu_x$ alloys with R → B19′ transformation, a decrease in ER occurs. Such a difference in resistivity behaviour also suggests that there is a different martensitic transformation sequence corresponding to a different type of resistivity change.

4.2. Effect of Cu addition on the *Ms* and T_R temperatures in $Ti_{50-x/2}Ni_{50-x/2}Cu_x$ alloys

Fig. 5a–c shows the *Ms* and T_R temperatures as a function of Cu and Fe concentrations for $Ti_{50-x/2}Ni_{50-x/2}Cu_x$, $Ti_{50}Ni_{50-x}Cu_x$ and $Ti_{50}Ni_{50-x}Fe_x$ alloys, respectively, in order to easily make a comparison. As can be seen in Fig. 5a, Cu additions in $Ti_{50-x/2}Ni_{50-x/2}Cu_x$ alloys shift both *Ms* and T_R to much lower temperatures with increasing Cu compositions. Mercier and Melton [2] demonstrated that even if the Cu in solid solution exceeds 30%, the *Ms* transformation temperature in $Ti_{50}Ni_{50-x}Cu_x$ alloys still changes very little and has a near constant *Ms* temperature behaviour, as partly shown in Fig. 5b. This feature is quite different from that shown in Fig. 5a. As mentioned in section 4.1, the transformation sequence of $Ti_{50-x/2}Ni_{50-x/2}Cu_x$ and $Ti_{50}Ni_{50-x}Cu_x$ alloys is quite different. However, the transformation sequence of $Ti_{50-x/2}Ni_{50-x/2}Cu_x$ and $Ti_{50}Ni_{50-x}Fe_x$ alloys is the same, i.e. B2 → R → B19′. Therefore, it is appropriate to choose the $Ti_{50}Ni_{50-x}Fe_x$ alloys for the comparison of concentration dependence of *Ms* and T_R temperatures, thus the results for $Ti_{50}Ni_{50-x}Fe_x$ alloys are shown in Fig. 5c [20].

In Fig. 5, $Ti_{50-x/2}Ni_{50-x/2}Cu_x$ alloys differ from $Ti_{50}Ni_{50-x}Fe_x$ alloys in the sense that the drop in *Ms* is comparable to that of T_R in the former alloy system; however, the drop in *Ms* is much greater (about three times greater) than that of T_R in the latter alloy system. In other words, the T_R temperatures in $Ti_{50-x/2}Ni_{50-x/2}Cu_x$ alloys are depressed quickly with increasing Cu content, whereas those in $Ti_{50}Ni_{50-x}Fe_x$ alloys are not depressed to the same extent of a much lower temperature with increasing Fe content. This elucidates the observed two nearly parallel lines of *Ms* and T_R curves for $Ti_{50-x/2}Ni_{50-x/2}Cu_x$ alloys in Fig. 5a and two nonparallel lines with one having a larger slope for $Ti_{50}Ni_{50-x}Fe_x$ alloys in Fig. 5c. Iron addition alloys can widen the temperature region in which the R-phase is stable while the current study of Fig. 5a for $Ti_{50-x/2}Ni_{50-x/2}Cu_x$ alloys shows no such effect. This phenomenon indicates that the substituted Cu atoms have a greater

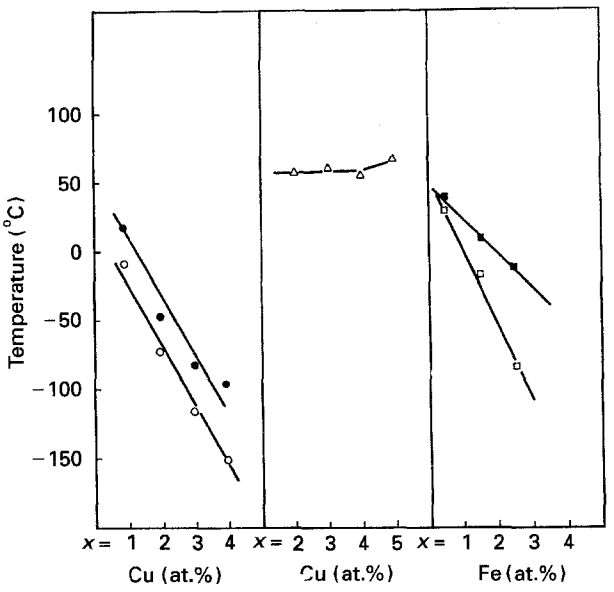

Figure 5 *Ms* and/or T_R temperature dependence of (a) Cu additions in $Ti_{50-x/2}Ni_{50-x/2}Cu_x$ alloys (○, *Ms*, ●, T_R); (b) Cu additions in $Ti_{50}Ni_{50-x}Cu_x$ alloys (△, *Ms*), (c) Fe additions in $Ti_{50}Ni_{50-x}Fe_x$ alloys (□, *Ms*, ■, T_R).

effect on increasing the R-phase and the martensite nucleation energies, therefore, both the T_R and *Ms* temperatures are depressed to a much lower temperature. However, in the case of Fe substituted alloys, the substituted Fe atoms have little effect on the nucleation energy of the R-phase but have a great effect on increasing the martensite nucleation energy and can cause the *Ms* temperature to depress to a lower temperature.

It is also well known that in as-quenched binary Ni-rich TiNi alloys, the *Ms* decreases with increasing Ni content – i.e., *Ms* decreases with increasing Ni/Ti ratio. In fact, the *Ms* temperatures of $Ti_{50-x/2}Ni_{50-x/2}Cu_x$ alloys also reveal this tendency: *Ms* decreases sharply with increasing (Ni + Cu)/Ti ratio. For example, the *Ms* temperature of an equiatomic TiNi binary alloy is about + 60 °C. By substituting 2 at % Cu for both Ti and Ni in $Ti_{50-x/2}Ni_{50-x/2}Cu_x$ alloy ([Ni + Cu]/Ti = 51/49), the *Ms* temperature becomes approximately − 71 °C (see Table I), which is almost the same as that of the as-quenched $Ti_{49}Ni_{51}$ alloy [20]. The above fact may suggest that Cu addition in $Ti_{50-x/2}Ni_{50-x/2}Cu_x$ alloys has an equivalent effect to increasing Ni in binary TiNi alloy. In other words, the substituted Cu atoms play a role more similar to Ni atoms than Ti atoms in TiNi alloys. This may further imply that the atom sites of Cu addition would prefer to occupy the position of Ni atom locations in the $Ti_{50-x/2}Ni_{50-x/2}Cu_x$ alloys. Employing the same proposal that Cu atoms prefer to occupy the Ni atom sites, but now in the $Ti_{50}Ni_{50-x}Cu_x$ alloys, instead of the $Ti_{50-x/2}Ni_{50-x/2}Cu_x$ alloys, it can also effectively account for the fact that large Cu substitutions for Ni result in a near constant *Ms* temperature behaviour [2, 3], for the reason that (Ni + Cu)/Ti ratio in $Ti_{50}Ni_{50-x}Cu_x$ alloys is preserved at a constant value of 1.

However, one recently reported study which employed electron channelling enhanced microanalysis (ALCHEMI) has shown that Cu atoms were located at both the Ni and Ti atom sites with nearly the same ratio in $Ti_{48.5}Ni_{48.5}Cu_3$ alloy [19]. Under such a situation, the Ni/Ti ratio in $Ti_{50-x/2}Ni_{50-x/2}Cu_x$ alloys will keep a constant value of 1, hence, the *Ms* temperature should also expect to be held almost constant, as with the same tendency shown in the $Ti_{50}Ni_{50-x}Cu_x$ alloys [2, 3], and not depressed to a much lower temperature as observed in the present study of $Ti_{50-x/2}Ni_{50-x/2}Cu_x$ alloys. The above description indicates that the effects of ternary Cu additions on the shift of *Ms* temperatures in terms of the site occupancies of Cu atoms cannot be accorded with the results of ALCHEMI [19]. As alluded to by Shabalovskaya [27], the changes of martensitic transformation temperatures may be closely related to electronic structure and state, such as the shift of the d-band, the d-band width and the site-projected densities of states at the Fermi level. Since the values of atomic radii, valence state, and ionic radii of Ni are different from Cu, the electronic structure and state of $Ti_{50-x/2}Ni_{50-x/2}Cu_x$ and $Ti_{50}Ni_{50-x}Cu_x$ alloys should be different from each other. However, without an exact understanding of the change of electronic nature caused by addition of elemental Cu, no further conclusion can be drawn, although there is a remarkable consistency in the changes of *Ms* temperatures with Ni content in the as-quenched Ni-rich TiNi alloys and with the Ni + Cu additions in the $Ti_{50-x/2}Ni_{50-x/2}Cu_x$ alloys.

5. Conclusions

Martensitic transformation sequences and transformation temperatures were investigated by means of electrical resistivity, DSC, X-ray diffraction and internal friction measurements in $Ti_{50-x/2}Ni_{50-x/2}Cu_x$ alloys. The martensitic transformation of $Ti_{50-x/2}Ni_{50-x/2}Cu_x$ alloys take place in B2 → R → B19′ two-stage sequences with x = 1–4 at %. When substitution exceeds 4 at %, the martensitic transformation does not occur even at very low temperature (liquid N_2). The results of B2 → R → B19′ transformation sequence suggest the addition of Cu in $Ti_{50-x/2}Ni_{50-x/2}Cu_x$ alloys assists the formation of the rhombohedral R-phase, which was suppressed in the $Ti_{50}Ni_{50-x}Cu_x$ alloys. The present study show that the effect of ternary Cu alloying element on the transformation sequence depends closely on the method by which Cu atoms substitute for Ti and/or Ni atoms, such as only Ni substituted in $Ti_{50}Ni_{50-x}Cu_x$ alloys, and Ti and Ni preserved equiatomic relation in $Ti_{50-x/2}Ni_{50-x/2}Cu_x$ alloys. The additions of Cu in $Ti_{50-x/2}Ni_{50-x/2}Cu_x$ alloys shift both *Ms* and T_R to much lower temperatures more rapidly than that of Fe in $Ti_{50}Ni_{50-x}Fe_x$ alloys. We suggest that Cu + Ni effects on the *Ms* temperature in $Ti_{50-x/2}Ni_{50-x/2}Cu_x$ alloys is similar as Cu + Ni effects in $Ti_{50}Ni_{50-x}Cu_x$ alloys and as Ni effects in as-quenched Ni-rich TiNi binary alloys. The reasons for the extremely low *Ms* and T_R

temperatures with small Cu addition in the $Ti_{50-x/2}Ni_{50-x/2}Cu_x$ alloys may be closely related to their electronic structure and state but are not yet fully understood.

Acknowledgements

The authors wish to acknowledge financial support for this research by the National Science Council (NSC), Republic of China, under the Grant NSC82-0405-E002-080. The authors also express their sincere appreciation to Mr C. S. Lin, Steel and Aluminium R&D Department, China Steel Corporation, for his great assistance in the internal friction measurements.

References

1. K. N. MELTON and O. MERCIER, *Met. Trans.* **9A** (1978) 1487.
2. O. MERCIER and K. N. MELTON, *ibid.* **10A** (1979) 387.
3. R. H. BRICKNELL, K. N. MELTON and O. MERCIER, *ibid.* **10A** (1979) 693.
4. R. H. BRICKNELL and K. N. MELTON, *ibid.* **11A** (1980) 1541.
5. T. TADAKI and C. M. WAYMAN, *Metallography* **15** (1982) 233, 247.
6. T. SABURI and S. NENNO, in Proceedings of the International Conference on Martensitic Transformations, Nova, Japan (1986) p. 671.
7. K. R. EDMONDS and C. M. HWANG, *Scripta Met.* **20** (1986) 733.
8. T. SABURI, T. TAKAGAKI, S. NENNO and K. KOSHINO, in Proceedings of the MRS International Meeting on Advanced Materials Shape-Memory Materials, Tokyo, Japan (1988) p. 147.
9. J. L. PROFT, K. N. MELTON and T. W. DUERIG, *ibid.* (1988) p. 159.
10. S. MIYAZAKI, I. SHIOTA, K. OTSUKA and H. TAMURA, *ibid.* (1988) p. 153.
11. T. SABURI, Y. WATANABE and S. NENNO, *ISIJ International* **29** (1989) 405.
12. W. J. MOBERLY, J. L. PROFT, T.W. DUERIG and R. SINCLAIR, *Material Science Forum* **56** (1990) 605.
13. K. TSUJI and K. NOMURA, *Scripta Met. Mater.* **24** (1990) 2037.
14. T. H. NAM, T. SABURI, Y. NAKATA and K. SHIMIZU, *Mater. Trans. JIM* **31** (1990) 1050.
15. T. H. NAM, T. SABURI, Y. KAWAMURA and K. SHIMIZU, *ibid.* **31** (1990) 262.
16. T. H. NAM, T. SABURI and K. SHIMIZU, *ibid.* **31** (1990) 959.
17. *Idem., ibid.* **33** (1991) 814.
18. Y. C. LO, S. K. WU and H. E. HORNG, *Acta Metall. Mater.* **41** (1993) 747.
19. Y. NAKATA, T. TADAKI and K. SHIMIZU, *Mater. Trans. JIM* **32** (1991) 500.
20. Y. C. LO and S. K. WU, unpublished work.
21. C. M. HWANG, M. MEICHIE, M. B. SALAMON and C. M. WAYMAN, *Phil. Mag.* **47A** (1983) 9.
22. Y. C. LO and S. K. WU, *Met. Trans.* **24A** (1993) 1205.
23. E. GOO and R. SINCLAIR, *Acta Met.* **33** (1985) 1717.
24. H. C. LIN and S. K. WU, *Scripta Met. Mater.* **25** (1991) 1295.
25. S. K. WU, H. C. LIN and T. S. CHOU, *Acta Metall. Mater.* **38** (1990) 95.
26. K. IWASAKI and R. HASIGUTI, *Trans. JIM* **28** (1987) 363.
27. S. A. SHABALOVSKAYA, in 'Proceedings of the Shape-Memory Materials and Phenomena-Fundamental Aspects and Applications', Boston, US, MRS Symposium Proceedings, Vol. 246, edited by C. T. Liu, H. Kunsmann, K. Otsuka and M. Wutting (MRS, 1992) p. 247.
28. S. MIYAZAKI and K. OTSUKA, in "Shape Memory Alloys", edited by H. Funakubo (Gordon and Breach Publisher, 1984) p. 116.

Received 2 July 1993
and accepted 8 September 1994